LAWRENCE
LIVERMORE
NATIONAL
LABORATORY

LLNL-CONF-425126

Creep Measurements on Plastic Bonded Explosives

B. J. Cunningham, F. J. Gagliardi, C. A. Hrousis, I. M. Darnell and S. Oh

March 4, 2010

14th International Detonation Symposium
Coeur d'Alene, Idaho, United States
April 11-16, 2010

Disclaimer

This document was prepared as an account of work sponsored by an agency of the United States government. Neither the United States government nor Lawrence Livermore National Security, LLC, nor any of their employees makes any warranty, expressed or implied, or assumes any legal liability or responsibility for the accuracy, completeness, or usefulness of any information, apparatus, product, or process disclosed, or represents that its use would not infringe privately owned rights. Reference herein to any specific commercial product, process, or service by trade name, trademark, manufacturer, or otherwise does not necessarily constitute or imply its endorsement, recommendation, or favoring by the United States government or Lawrence Livermore National Security, LLC. The views and opinions of authors expressed herein do not necessarily state or reflect those of the United States government or Lawrence Livermore National Security, LLC, and shall not be used for advertising or product endorsement purposes.

Creep Measurements on Plastic Bonded Explosives

Bruce Cunningham, Franco Gagliardi, Constantine Hrousis, Ian Darnell, and Sejin Oh

Lawrence Livermore National Laboratory
P.O. Box 808 L-282
Livermore, California

Abstract. We report on the development of hardware and methodologies used to measure creep and recovery in PBX materials. Specific emphasis is on measurements involving the insensitive high explosives (IHEs) including LX-17-1 and PBX-9502. The work described includes constant-stress, uniaxial creep performed at temperatures ranging from as low as 24˚C, up to 70˚C, with stresses ranging from approximately 1.7 to 5.4 Mpa. In addition to uniaxially loaded, unconfined creep measurements, we also report on experiments in which the materials tested were under a state of lateral confinement. Several sensor types are used in our experiments, so that load-creep-unload-recovery strain histories are derived through hybridization of the data from the two sensor types. Prior to the onset of material failure, strain-time plots for these materials have been shown to be accurately fit using simple log expressions. This serves to facilitate extrapolation and assists in the creation of computer-based models. In addition to compression creep, we also discuss our early efforts directed toward measuring creep in tension using digital image correlation (DIC).

Introduction

Within systems that contain plastic bonded explosives (PBXs), individual components may experience a variety of temperature and stress conditions. As a consequence, and depending on the material's state of confinement, the explosive constituents may undergo a slow process of deformation. It is this slow deformation, taking place over perhaps as long as several decades, that is the particular focus of our ongoing experimental effort reported here.

For the past several years we have been developing instrumentation to accurately measure creep strain in plastic bonded explosives. The purpose of this effort has been to enhance our understanding of creep as it occurs in explosive systems, and specifically, to provide the Livermore modeling community with the data necessary to build and test creep-predictive computer based system models[1]. Although the test instrumentation developed has been used to generate data on a number of energetic materials, the bulk of our work has focused on the insensitive high explosives (IHEs). The materials that we have tested primarily include compactions made from LX-17-1 and PBX-9502. Both of these explosives are highly filled polymers consisting of a mixture of triamotrinitrobenzene (TATB) and chlorotrifluoroethylene/vinylide fluoride (KEL-F 800). Kel-F 800 has a glass transition temperature

(Tg) of between 25 and 30˚C[2]. The two PBXs differ in their relative weight percents of binder (7.5% for LX17-1 and 5% for PBX 9502) and in the manner in which their crystalline energetic content is formulated. These materials are most often compacted at elevated temperatures using pre-mixed beads of enegetic and binder called "prills". Compacting is usually performed at temperatures around 105˚C and under pressures that are typically between 135 and 210 MPa. Compacting may be achieved in several ways, most commonly through the use of steel dies and plungers, or hydrostatically using pressurized liquids. In the case of hydrostatic compaction, finished part shapes are generally derived through the subsequent machining of rough pressings or billet pressed material.

The majority of our work, to date, has focused on the measurement of creep in compression[3]. For these tests, samples are cylindrical, and usually machined from hydrostatic pressings. They measure a nominal 12.7 mm in diameter and 25.4 mm long. As might be expected from compactions consisting of a crystalline energetic that is bound by the copolymer Kel-F 800, rates of creep for these materials are highly stress and temperature dependant[4]. Figure 1 shows a photograph of a standard compression sample.

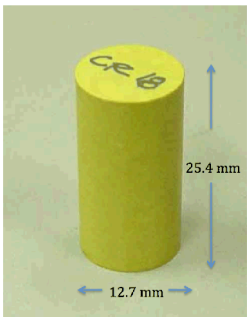

Figure 1 – Creep Compression Specimen

Creep measurement in highly filled polymers presents, in general, special challenges. The relatively long time periods required to adequately capture the behavioral characteristics associated with creep places stringent requirements on the long-term stability of the sensors used to monitor strains. Since the creep rates encountered can be very slow, particularly at temperatures below the glass transition temperature, the sensors employed must possess a high degree of precision as well. Further, because the creep rates exhibited by the material are sensitive to small temperature fluctuations, testing of this type demands steady temperature control during testing.

Hardware and Test Methodology Development

Several early attempts at long-term creep measurement using gages applied directly to the specimen were unsuccessful due to problems with gage drift and to creep at the gage and specimen interface. Following these first attempts, a decision was made to avoid some of our past problems by opting not to use directly applied contact sensors. Instead, we chose to use as our primary, long term creep monitoring method, the measurement of inferred strain as determined by the relative motion of two loading platen surfaces that are in direct contact with the specimen and that are the source of the applied stress. While this technique has some drawbacks, the method's inherent long-term stability has proven, overall, to yield very satisfactory results.

In addition to choosing a primary approach to measurement, an acceptable design for our fixture, as well as the down-selection of a displacement sensor to measure long-term creep and recovery, was also necessary. Extensive evaluations of three candidate sensor types, and of two different creep fixture designs, were performed. Displacement sensors evaluated included fiber-optic, capacitance, and linear variable differential transformer (LVDT) gages. Our criteria for sensor down-selection included:
1) signal stability over long time periods, 2) precision, 3) relative insensitivity to temperature fluctuations, 4) ease of implementation, and 5) to a somewhat lesser extent, cost. After considerable testing, we found that our fiber-optic gage suffered from instability in its output electronics that were attributable to changes in the environmental (room) temperature. The capacitance gage was stable and offered, potentially, the greatest precision of the three sensors. However, it was quite expensive and somewhat difficult to

implement. In the final analysis, we found the best choice for our application to be LVDTs, which were quite stable and insensitive to temperature change, easy to implement, adequately precise, and, as a bonus, the least expensive of the three sensor types.

Two quite different fixture designs were built and evaluated in parallel. The first design (Design 1) used a single sensor, center mounted, that monitored movement of a specimen applied Invar rod and cap. The rod and cap rested on the top of the cylindrical specimen. Rods attached to the cap, transferred a compressive load from a hanging weight, through a lever-derived force multiplier system, and finally to the specimen. This design also incorporated an aluminum tubular support for the capacitance gage. The machined length of the aluminum tube was to be chosen precisely so that small amounts of sample growth and shrinkage, attributable to very small temperature fluctuations within the test chamber, could be mechanically "filtered" from the data. For the metrology aspects of device to be effective, the tube length had to be tailored to the specimen material's CTE, at the specific test temperature. The latter was necessary because the thermal expansion behavior of the material in question is markedly temperature dependent. This design also included a tightly sealed thermal enclosure surrounding the sample and its metrology tube. A heater-tape situated between the thermal enclosure and outermost insulating jacket served as the heating source.

The second fixture design (Design 2) is essentially a modification of our standard precision compression cage (see Figure 2). In this design, three LVDT bodies containing windings are peripherally affixed at a 120-degree spacing to the upper loading platen of the cage. Rods, with LVDT cores at their ends, are attached to the lower platen in corresponding positions, so that as relative motion occurs between the platens, that same motion also occurs between the LVDT bodies and their cores. The variable output from the three gages are converted to displacements and then recorded individually and also averaged to yield an average displacement. The heat source in this design is a conventional, medium wattage light bulb situated inside the insulated space containing the fixture. Different load levels can be applied by changing the weights that are attached, by chain, to the fixture and hang directly below the insulated cell. A variant of this particular design also provided for intrinsic metrology correction via adjustable, Invar based linkages between the lower platens and the cores. However, this feature has not been routinely implemented as it has generally been found to be unnecessarily complex, since the

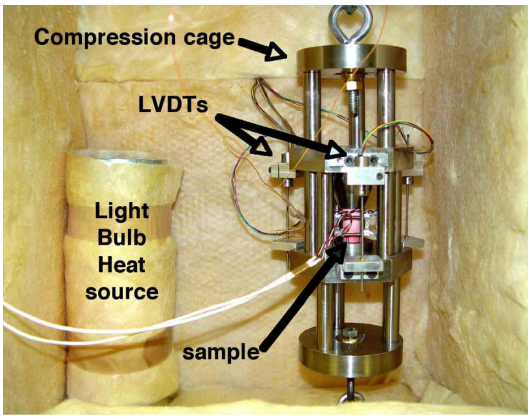

Figure 2 – Creep Fixture in Cell, Design 2

noise in the data arising from small temperature fluctuations could be corrected for by averaging.

A considerable period of assessment revealed that our first design, Design 1, suffered from several problems, including imprecision in the load train. Other problems included rotation (tilting) of the rod-cap during testing that affected the strain data, as well as inaccessibility to the sample. In addition, the heating system was found to be over-insulated, resulting in long correction response times. The lack of accessibility to the sample interfered with our ability to make short-term measurements using extensometers. Such measurements ultimately proved important in determining strain changes during load-up and unload, and in providing data verification. Further, our experience has shown that averaging from multiple gages has historically given better results than have single gage measurements, and we believe this to be the case here as well.

Having chosen our gage and our basic fixture design, we completed the construction of multiple stations (see Figure 3). Each station is comprised of: 1) a compression fixture with three averaging LVDT gages attached, 2) a light bulb heat source,

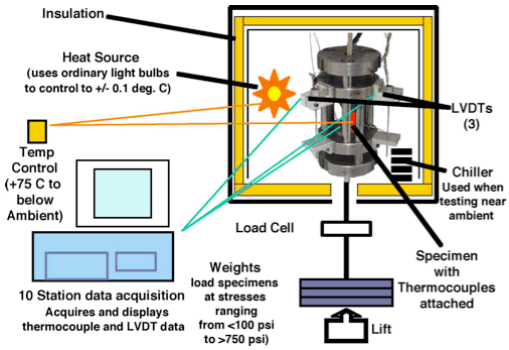

Figure 3 – System Schematic

3) insulation, 4) three digitizing LVDT readouts, 5) a weight system, 6) a temperature control system, and 7) an overall computer based software system for data acquisition and test control. The computer and software system is designed to accommodate the simultaneous temperature regulation, data monitoring, and data acquisition of as many as ten separate creep stations Each station can be loaded and unloaded individually, and can also be run independently, at different loads and temperatures.

As designed, our system provides an effective near 1 microstrain resolution. Data acquisition rates (with all stations running simultaneously) can be software selected, beginning with a rate as high as1 data record every 15 seconds. Each record includes individual displacement data from the three LVDTs, along with temperature data from the sample-mounted thermocouple. Temperature control is to approximately +/- 0.1˚C. In addition, displacements from the individual LVDTs are measured, converted to strains, and recorded simultaneously and independently. Data from the extensometer pairs (see text below) is acquired on a separate system running independently.

A Description of the Data Typically Acquired

In the bulk of our work we have concerned ourselves primarily with creep deformations that take place at relatively low loading levels, so that the onset of failure does not generally occur within the test period.

In our experiments that measure only creep behaviors that take place prior to the onset of failure, our usual creep and recovery test can be thought of as having four distinct phases (see Figure 4). In phase 1, referred to here as "**load up**", the load is applied to the specimen. In this first, brief phase, the strain response of the specimen depends on, among other things, the rate at which loading occurs (and consequently, the strain rate). Knowing the applied stress, the test temperature, as well as the effective average strain rate during load application, the strain achieved during this phase may be predicted from independently acquired strain controlled stress-strain curves. This provides a means for crosschecking this particular portion of the test.

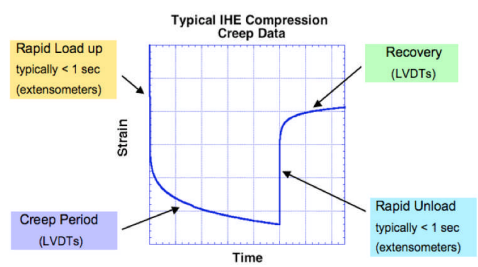

Figure 4 – Four Stages of a Basic Creep Test.

In phase 2, **creep**, additional time-dependant strain is added to the strain that occurred during load application. The strain rate at any given instant in the process depends on several factors, including stress on the specimen, the specimen temperature, and on the time since load was applied. Except for the case where the load level is sufficient to induce the onset of failure in the specimen during the test, the creep strain rate typically decreases with time.

In phase 3, "**unload"**, the weight is removed and a rapid, and to at least some degree partial, recovery (elastic spring-back) occurs. The amount of spring-back depends on the stress that had been applied, the test temperature, and on the time of load application.

In phase 4, "**recovery"**, the sample slowly reclaims, over time, a portion of its length that was lost during loadup and creep. Following recovery, non-recoverable compressive strain (residual plastic strain) will remain in the specimen. Once again, the amount of permanent residual strain is a function of stress, temperature, and the amount of creep time.

Post-Test Data Processing

With the LVDT system, strain measurement is not made directly on the sample, but rather is inferred from the relative motion of platens in contact with the sample ends. We have found that, during the initial "loadup" phase and also during "unload", extra or "false" strain is recorded by the LVDTs. This false strain is the consequence of the small amount of space between the platens and specimen ends closing when force is applied, or opening during load removal. This effect is greatest when specimens are imperfectly machined (they have non-flat and / or non-parallel ends). False strain is also a greater problem with tests that are performed at cooler temperatures (resulting in poorer sample end compliance) and at lower stresses (there is greater percentage error).

The problem of false strain is largely overcome through the use of extensometer pairs, attached directly to the specimen, that are used to measure strain only during the very short-term "loadup" and unload periods. In addition to providing an accurate measurement of these brief events, the technique provides the added benefit of allowing very higher speed (100 data points per second) data acquisition rates in circumstances where higher digital resolution is important. During the creep and recovery phases, the LVDT data is acquired, typically, at a rate of four data points per minute, which is perfectly adequate for these two phases of the test.

To insure accuracy, gravitational load levels are adjusted after dry-loading the system with a calibrated load cell in place of the specimen. Thermocouples are checked against calibrated temperature wells, LVDTs and extensometers are checked using a digital Boeckeler® head fitted with an electronic readout. Strain output from the three LVDTs is verified by inserting several standards, whose lengths deviate slightly from that of the 2.54 cm long specimen, and noting the differences in indicated relative LVDT positions.

Prior to load application, the ends of the specimen are lubricated, and the specimen is placed in its test fixture, with extensometers and thermocouples attached. For safety purposes, two thermocouples are used – one to monitor the temperature, and one, for safety reasons, that is attached to an over-temperature controller set to trip at slightly above the test temperature. Within the insulated chamber, the PDF-regulated specimen temperature is ramped to the target value over a period of several hours, and when temperature stability is achieved, the load is applied by dropping the weight support tray situated below the chamber. After a preselected time period, the load is removed, allowing recovery to occur.

Upon completing a test, the data from the two gage types is combined by mathematically shifting the average LVDT strain to match the strain measured by the extensometer at "loadup". Likewise, the portion of the data beginning with, and subsequent to, unload is also shifted to match the unload strain with that which was measured by the extensometer at the time of unload. Although the extent of disagreement between the two gage sets varies, the average loadup and unload strain shown by the LVDTs is invariably greater than that shown by the extensometer pair. This is because the loadup strain measured by the LVDTs always includes some amount of false strain that is attributable to relative motion between the loading surfaces and the specimen ends.

Results and Discussion: Uniaxial Compression Data

Lightly Loaded IHEs

For lightly loaded specimens (those for which the loading and temperature histories are such that the material does not reach the onset of failure within the test period), the IHEs exhibit creep behavior in which creep strain accumulates but creep rates gradually slow with time. During creep, both reversible and irreversible strain (permanent damage) accumulates. Irreversible damage is evidenced as a constituent present in the recovery data portion of the creep tests to follow.

Figure 5 shows typical creep and recovery data from three previously untested PBX 9502 samples in which the specimens were loaded and crept for four weeks, and then allowed to recover for eight. The plots show strain as a function of time, for all three samples, each of which was tested at 50 ˚C. The stress loadings for the three tests were 1.7, 3.4, and 5.4 MPa respectively. Note that the indicated creep strains, recovery strains and rates, and the implied residual (non recoverable) strain, all increase with load stress.

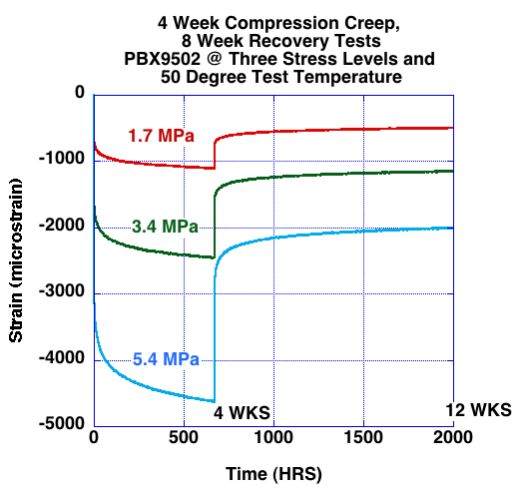

Figure 5 – Example Creep and Recovery Data.

An important finding of our work has been that, prior to the initiation of collapse, under conditions of fixed stress and temperature, the IHEs exhibit strain-time behaviors that may be accurately fit by simple log expressions of the form:

$$strain = a+b*log(time) \qquad (1)$$

This behavioral characteristic applies both to the creep and to the recovery phases of the test. Recognition of this phenomenon has helped to simplify the modeling process considerably. Relative creep rates may be expressed simply in terms of the multiplier "b" as it appears in the strain-time expression shown above. See Figure 6.

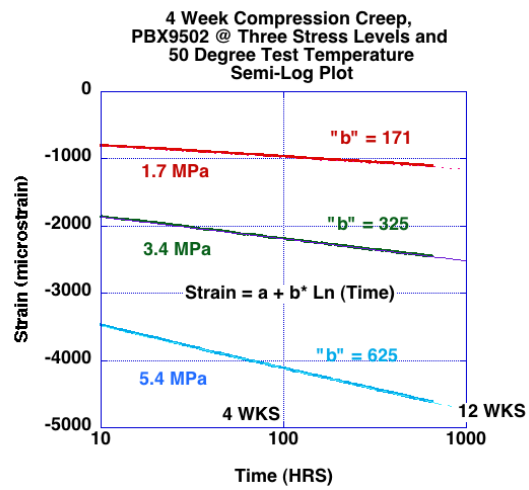

Figure 6- Semi-Log Plots of the Data Shown in Figure 5. Note the "b" Slope Values.

Because semi-log plots of the individual creep or recovery phases are inherently linear, long term predictions based on extrapolations are easily arrived at. See Figure 7.

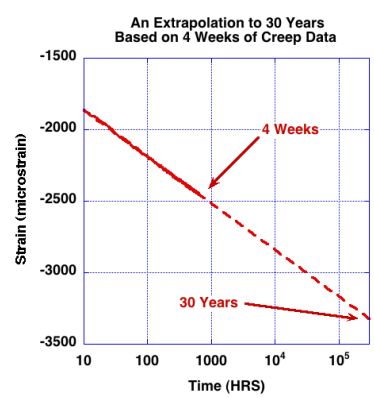

Figure 7 – A long-Term Creep Extrapolation.

Heavily Loaded IHEs

As uniaxial compression creep in the IHEs continues, eventually a point will be encountered where the strain-time curve infects, and creep rates begin to accelerate (see Figure 8). For a lightly loaded material, the time to reach the onset of failure will often be sufficiently long that the collapse phase of the uniaxial creep process is not a concern. In the case of the more highly loaded material tests, collapse will ensue and the damage approaching failure becomes progressively more extreme so that phenomena such as prill separation may occur. In the end, internal material damage becomes so extreme that the specimen fractures catastrophically. See Figure 8.

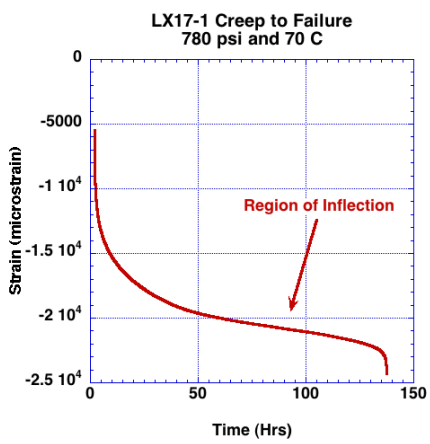

Figure 8 – Strain Data from a Specimen Crept to Failure.

More Complex Scenarios

One can, of course, envision an endless number of complex sequences involving multiple mixed load-creep-unload-recovery events. During sequences such as this, temperatures and loads could vary within one or many sub-events. The final strain state of the material in question would, of course, be dependent on the materials complete stress and thermal histories. To further complicate the problem, tensile stress, as well as multi-axial stress states are also quite possible.

In an effort to produce additional data needed to test our creep model under more complex creep scenarios, we have performed other, more elaborate creep experiments, including those in which we: a) loaded and unloaded the specimens multiple times over extended periods of time, b) changed loading during the test, and c) changed temperature during the test. In this latter case, because our LVDT based measurement system provides consistent, calibrated output only when the temperature is held constant, it was necessary to obtain specific system correction data for the test. This was done by duplicating the temperature transition phase of the experiment while using a titanium silicate (a very low thermal expansion material) specimen as a substitute for the IHE. The data so derived allowed us to correct for errors in the strain measurement that were the consequence of temperature change effects on the system itself. See Figure 9.

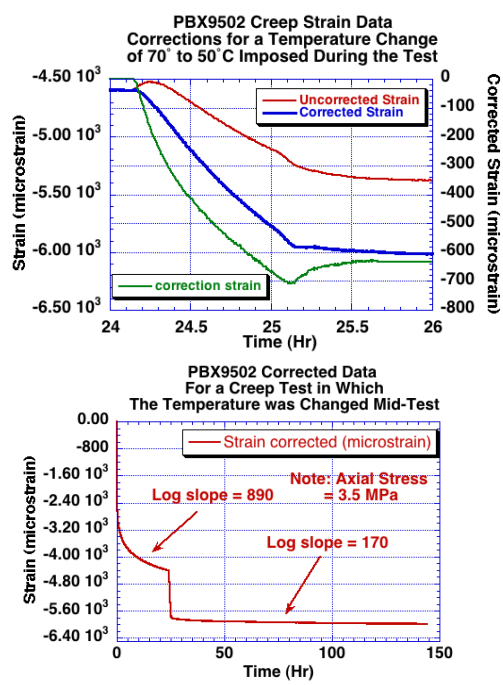

Figure 9 – Creep Data Corrected for a Mid-Test Temperature Change From 70 to 50˚C.

Confined Creep Testing

Multiaxial stress states more accurately represent real world system conditions than do uniaxial stress states. Consequently, in ongoing work, we devised methods to perform compressive creep experiments on IHEs under various levels of lateral confinement[5]. To accomplish these more complex measurements, additional hardware was designed and implemented. See Figure 10. The new hardware, which is used in conjunction with the existing creep fixtures, allows a controlled confining stress to be applied to the periphery of the creep sample during testing. In detail, confinement is achieved through the use of a small pressure vessel that is connected to a nitrogen gas bottle and regulator. When pressure is turned on,

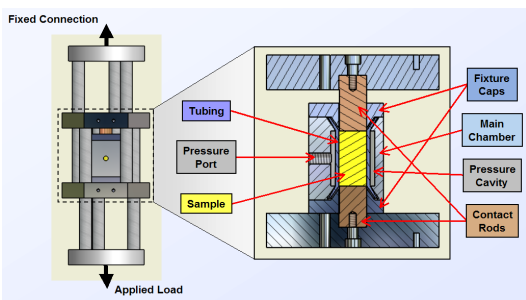

Figure 10 – Creep Confinement Fixture

gas is introduced into the vessel so that a tubular bladder surrounding the specimen is compressed, squeezing the specimen. With the introduction of confinement, the potential matrix of experiments becomes larger and more complex. For these tests, independently controlled variables include the level of confinement, in addition to the magnitude of the applied axial stress and the test temperature. See Figure 11. In all, 25 experiments were performed in a matrix of confined creep tests performed on LX-17-1. An initial analysis of the confined creep data did not immediately yield insights into the nature of interrelationships between confinement and axial stress, temperature and creep rate. However, closer scrutiny of the data revealed that a significant ordering does,

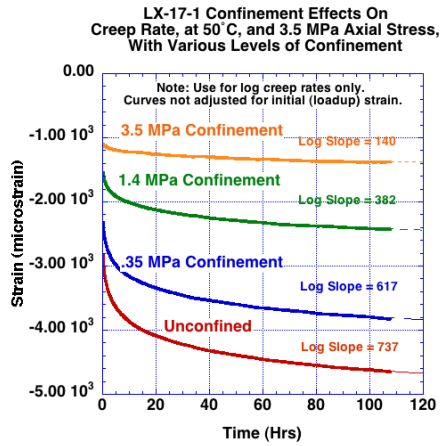

Figure 11 – Confinement Effects on LX17-1 at 50˚C.

in fact, exist. When creep rates for experiments performed at a specific temperature are plotted as a function of the difference between the axial stress and the confining stress (*axial stress-confining stress*), all data points acquired at that temperature, including those from earlier zero-confinement pressure tests, tend to fall on a single curve. There is, however, a notable inconsistency. In the case where the axial and confining stress are equal (axial stress minus confining stress = 0) the rule stated above would predict a creep rate that is a constant and independent of the level of axial and confining stresses. In fact, when the applied stresses are equal, and therefore the stress condition is effectively hydrostatic, the material will still creep. Creep occurs under hydrostatic conditions, in spite of the fact that the material in the specimen was initially compacted using pressures on the order of 140-200 MPa. This is because the theoretical maximum density is never fully achieved, and so some voids will always be present. As a result, further densification is still possible and the rate of densification, although quite slow, increases as the level of hydrostatic pressure increases. See Figure 12.

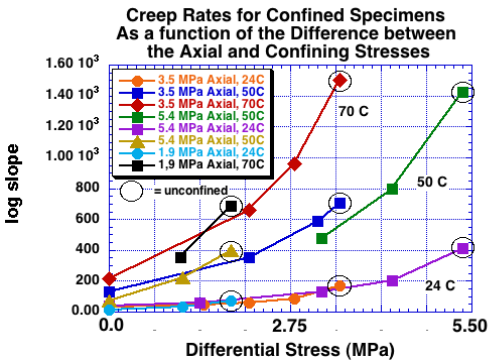

Figure 12 – Creep Rates as a Function of the Axial Stress minus the Confining Stress.

Initial Work on Tensile Creep Measurement

We would like to perform experiments to measure IHE creep in tension as well as in compression. Current efforts have been directed towards measuring PBX tensile creep using standard dog bone shaped specimens (Figure 13).

Figure 13 – Standard Tensile Specimen.

Tensile creep measurement on specimens of this type presents special challenges. We had previously determined that that the application of gages (such as extensometers) directly to the PBX specimens, often produce results that are unsatisfactory over long test periods. Error sources when using this type of gage include electronic drift, sensitivity to temperature changes and to changes in heat transfer conditions at the gage, as well as possible localized creep at the extensometer knife and specimen interface. Since we had already been successful measuring compression creep strain by inference, measurement by inference seemed, at first, to be a reasonable approach to what appeared to be a similar problem. Unfortunately, our initial efforts in this regard have yielded results that are inconsistent. With this approach, a significant problem arises from the tensile specimen's use of conical ends for gripping. In the case of compression creep, the specimen gage length is clearly defined (it is the full length of the cylinder). In the case of tensile specimens, creep, in addition to taking place within the constant diameter shank region, may also occur within the cone volumes as well. This fact make's it quite difficult to establish a clearly defined region in which creep is taking place. We have had some success using "effective" gage lengths estimated by performing short-term tests in which we compare extensometer strain measurements to those inferred from LVDTs attached to the tensile fixture. However, ongoing uncertainties related to this particular issue, as well as uncertainties associated with early failure arising from stress concentrations near the sample grip regions, have motivated us to look at other approaches to tensile strain measurement.

One of the more promising approaches includes the use of a non-contact optical strain-measurement method, specifically DIC (digital image correlation)[6]. This technique has the advantage of producing strain maps over a large area of the sample surface. Although we are in the early stages of this work, we are encouraged by results to date. Figure 14 shows a composite image illustrating the setup for a cell that has been modified to accept our standard tensile fixture as well as a DIC stereo camera pair. Figure 15 shows some example DIC acquired short-term creep data derived from a test in which the sample was aggressively loaded to 500 psi and tested at 50˚C. In this particular test, failure in the specimen occurred in under 2 hours. Although this is a short creep test, the data resolution appears to be quite good, and the technique has the benefit of yielding data on loading uniformity as well as in areas of stress concentration. In addition, the technique provides us with the added ability to track strain recovery on the surfaces of the separated parts of the broken specimen, post-fracture. A drawback to this experimental approach currently is that we are limited to viewing only the forward portion of the specimen. Efforts to correct for this problem,

and to further develop this methodology in general, are ongoing.

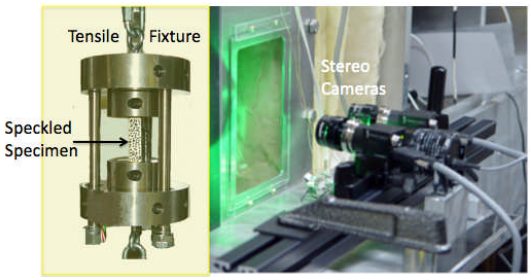

Figure 14 – Creep Measurement Using DIC.

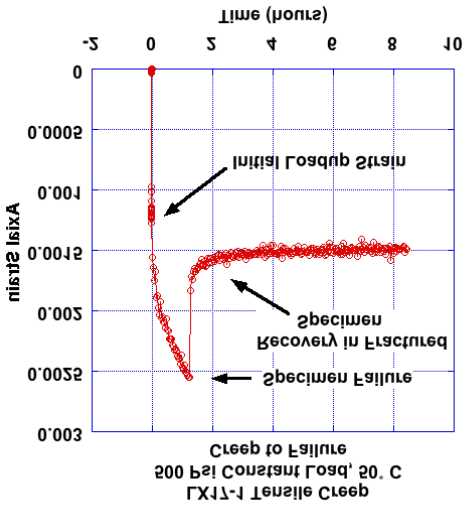

Figure 15 – DIC Derived Data From a Short-Term Tensile Creep to Failure Test.

This work was performed under the auspices of the U.S. Department of Energy by Lawrence Livermore National Laboratory under Contract DE-AC52-07NA27344.

References

1. See Darnell, I.M. et. al., in this volume

2. Rizzo, H. F., Humphry, J. R., and Kolb, J. R., "Growth of 1,3,5-Triamino-2,4,6-Trinitrobenzene (TATB). II. Control of Growth by Use of High Tg Polymeric Binders", UCRL 52662, March 7, 1979.

3. Gagliardi, F. J. and Cunningham, B. J., "Creep Testing Plastic-Bonded Explosives in Uniaxial Compression", SEM XI International Conference on Experimental and Applied Mechanics, Orlando, Florida, June 2-5, 2008

4. DoBratz, B. M. (Ed.), "*Lawrence Livermore National Laboratory Explosives Handbook*", Mechanical Properties, UCRL-52997 (Revised Jan. 1985).

5. Cunningham, B. J., and Gagliardi, F. J., "Confined Creep testing of Plastic Bonded Explosives", 2009 SEM Annual Conference on Experimental Mechanics, Albuquerque, New Mexico, June 1-4, 2009.

6. Sutton, M. A., Orteu, J. J., and Schreier, H. W., "Image Correlation for Shape, Motion and Deformation Measurements", Springer, New York, 2009.